Supplementary File S1

Pangenome-Scale Mathematical Modelling of ANAMMOX Bacteria Metabolism

Roman G. Bielski and M. Ahsanul Islam

Department of Chemical Engineering, Loughborough University, Leicestershire,

LE11 3TU, England, United Kingdom

Author emails: R.G.Bielski@lboro.ac.uk and M.Islam@lboro.ac.uk

Table of Contents

List of Figures

Model Details

Table S1: General features of iRB399

Genes	
Total number of protein-coding genes	1432
Total number of open reading frames included in the model	399
Genes from *Ca. Kuenenia stuttgartiensis*	344
Genes from the rest of the pangenome	55
Genes involved in more than one reaction	62
Genes excluded from the model from *Ca. Kuenenia stuttgartiensis*	1173
Intra-System Reactions	
Total number of model reactions	408
Gene-associated reactions	249
Non-gene associated reactions	155
Exchange reactions	
Total number of exchange reactions	44
Input-output reactions	407
Biomass Demand reaction	1
KEGG database Metabolites	386
Non-KEGG database metabolites	6 in biomass (#?) intermediaries
Total number of metabolites	416
Number of Extracellular Metabolites	33
Number of Biomass Metabolites	62
Reaction sources	
Genome Annotation	249
Gap filling	143

Table S2:MEMOTE[1] report generated from iRB399.

Consistency	
Mass Balance	84.3%
Charge Balance	86.0%
Metabolite Connectivity	99.5%
Unbounded Flux In Default Medium	91.6%
Metabolite Information	
Unique Metabolites	426
Duplicate Metabolites in Identical Compartments	2152
Metabolites without charge	0
Metabolites without formula	0
Medium Components	20
Reaction Information	
Purely metabolic Reactions	373
Purely Metabolic Reactions with Constraints	28
Transport Reactions	48
Transport Reactions with Constraints	13
Matrix Conditioning	

Ratio Min/Max Non-Zero Coefficients	0
Independent Conservation Relations	28
Rank	398
Degrees Of Freedom	52

Biomass Objective Function

Table S3: Macromolecular composition of the biomass objective function in iRB399.

Metabolite Class	**% w/w composition**
Protein	60.0’
DNA	4.03*
RNA	5*
Lipid	12.6’ (calculated as what is left over)
Ion	3
Metabolites	1.94**
Cell wall Components	13.97*
Total	100

‘Experimental value *Estimated value **composition from Bacillus Subtillis [2].

Table S4: Protein coding sequences in *Ca. Kuenenia stuttgartiensis* from RefSeq assembly accension GCF_900232105.1.

Amino Acid	Number	%	Amino Acid	Number	%	Amino Acid	Number	%
A (L-Alanine)	74959	6.78	I (L-Isoleucine)	91053	8.24	R (L-Arginine)	52771	4.77
C (L-Cysteine)	15250	1.38	K (L-Lysine)	83949	7.60	S (L-Serine)	67585	6.12
D (L- Aspartic acid)	56769	5.14	L (L-Leucine)	103050	9.32	T (L-Threonine)	59167	5.35
E (L-Glutamic acid)	77305	6.99	M (L-Methionine)	26989	2.44	V (L-Valine)	70747	6.40
F (L-Phenylalanine)	50127	4.54	N (L-Asparagine)	51548	4.66	W (L-Tryptophan)	11642	1.05
G (Glycine)	74657	6.76	P (L-Proline)	41157	3.72	Y (L-Tyrosine)	39871	3.61
H (L-Histidine)	23485	2.12	Q (L-Glutamine)	33098	2.99			

The protein dry mass composition of the cell is 60% which corresponds to 50g per litre of biomass [3].

Table S5: Calculation of amino acid contribution to biomass in one gram of dry cell weight (DCW).

Amino acid	ORF	prevalence %	MW	%P*MW	% (By weight)	mmol/gDCW
A (L-Alanine)	74959	6.78	89.10	604.32	4.63	0.31
C (L-Cysteine)	15250	1.38	121.10	167.10	1.28	0.06
D (L- Aspartic acid)	56769	5.14	133.10	683.69	5.23	0.24
E (L- Glutamic acid)	77305	6.99	147.10	1028.93	7.88	0.32
F (L-Phenylalanine)	50127	4.54	165.20	749.29	5.74	0.21
G (Glycine)	74657	6.76	75.10	507.32	3.88	0.31

H (L- Histidine)	23485	2.12	155.20	329.80	2.52	0.10
I (L- Isoleucine)	91053	8.24	131.20	1080.92	8.27	0.38
K (L- Lysine)	83949	7.60	146.20	1110.53	8.50	0.35
L (L- Leucine)	103050	9.32	131.20	1223.35	9.36	0.43
M (L- Methionine)	26989	2.44	149.20	364.35	2.79	0.11
N (L- Asparagine)	51548	4.66	132.10	616.14	4.72	0.21
P (L- Proline)	41157	3.72	115.10	428.63	3.28	0.17
Q (L- Glutamine)	33098	2.99	146.10	437.54	3.35	0.14
R (L- Arginine)	52771	4.77	174.20	831.78	6.37	0.22
S (L- Serine)	67585	6.12	105.10	642.72	4.92	0.28
T (L- Threonine)	59167	5.35	119.10	637.62	4.88	0.25
V (L- Valine)	70747	6.40	117.20	750.24	5.74	0.29
W (L- Tryptophan)	11642	1.05	204.23	215.14	1.65	0.05
Y (L- Tyrosine)	39871	3.61	181.20	653.71	5.00	0.17
	1105179	100.00		13063.13		

Table S6: DNA contribution to the biomass objective function in iRB399

DNA	Count (all ORFs)	% Prevalence	MW	%P*MW	% (By weight)	mmol/gDCW
dATP	1301484	0.295	487	143.9	29.8	0.01835683
dCTP	903309	0.205	462.99	94.9	19.7	0.012740756
dGTP	907153	0.206	503	103.6	21.5	0.012794974
dTTP	1294235	0.294	477.99	140.4	29.1	0.018254586
Totals	4406181	1		482.7253099	100	

Table S7: Ion contribution to the biomass objective function in iRB399 [2].

Component	% w/w	MW (g/mol)	g/gDCW	mmol/gDCW*
K^+	86	39.1	0.0259	0.663
Mg^{2+}	7.7	24.3	0.00232	0.956
Fe^{3+}	0.6	55.9	0.000181	0.00323
Ca^{2+}	0.4	40.1	0.000121	0.00301
Phosphate	4.3	96.0	0.00130	0.0135
Diphosphate	0.5	174.9	0.000151	0.000862
Sum	99.5		0.03	

The overall charge within the cell was made to be neutral according to the law of electroneutrality.

Table S8: Lipid profile of an ANAMMOX cell. FA, fatty acid; mE, monoether; diE, diether; Lad., ladderane; amxs. Lipid composition of cell wall and anammoxosome [4].

Lipids after base hydrolysis	Intact cells	Amxs with riboplasm	Isolated amxs
isoC14 FA	1.7	1.8	1.8
C14:0 FA	7.4	7.8	7.6

isoC16 FA	3.2	2.9	3.2
C16:0 FA	12.3	10.0	12.8
10MeC16 FA	10.3	11.2	11.6
C18 lad. FAs	6.4	7.3	7.7
C20 lad. FAs	15.8	17.9	17.6
Squalene	2.3	2.3	2.6
Lad. Glycerol mE	29.0	29.3	27.4
Diplopterol	0.5	0.3	0.4
isoC14/C20 lad. Glycerol diE	2.4	2.0	1.5
C14/C20 lad. Glycerol diE	5.2	4.5	3.3
C16/C20 lad. Glycerol diE	2.0	2.0	1.4
Bacteriohopanetetrol	1.5	0.7	2.1

Table S9: Calculation of lipid contribution to biomass objective function in iRB399.

Component	Content %	MW (g/mol)	g/gDCW (12% of DCW)	µmol/gDCW*
isoC14 FA	1.7	228.376	0.00214	9.379
C14:0 FA	7.4	228.376	0.00932	40.82
isoC16 FA	3.2	256.43	0.00403	15.72
C16:0 FA	12.3	256.43	0.01550	60.43
10MeC16 FA	10.3	270.5	0.01298	47.98
C18 lad. FAs	6.4	274.4	0.00806	29.39
C20 lad. FAs	15.8	302.5	0.01991	65.81
Squalene	2.3	410.73	0.00290	7.056
Lad. Glycerol mE	29	367.58	0.03654	99.41
Diplopterol	0.5	428.7	0.00063	1.470
isoC14/C20 lad. Glycerol diE	2.4	563.58	0.00302	5.362
C14/C20 lad. Glycerol diE	5.2	563.95	0.00655	11.62
C16/C20 lad. Glycerol diE	2	592.004	0.00252	4.257
Bacteriohopanetetrol	1.5	546.86	0.00189	3.456
Bacteriohopanetetrol* (in model)	1.5	428.7 (same as Diplopterol)	0.00189	4.409

*Bacteriohopanetetrol mass is considered as Diplopterol since the Bacteriohopanetetrol biosynthesis pathway is missing.

Table S10: Muropeptide contribution to the biomass objective function determined by mass spectrometry[5].

Muropeptide	Relative abundance %	$[M + H]^+$ theoretical	$[M + H]^+$ determined	Difference (theo-det)	Basis % corrected abundance	mmol/ gDCW
M3	31.5	871.38	871.37	0.01	47.4	0.759
M4	5.8	942.41	942.36	0.05	8.72	0.013
M2	6.9	699.29	699.27	0.02	10.4	0.021
D43	22.3	1794.77	1794.70	0.07	33.5	0.026

D44*	5.7	1865.81	ND	-		
-*	10.1	-	ND	-		

*The relative abundances do not sum to 100% and the measurement for D44 and the unknown sixth muropeptide cannot be used so only the first four rows on the table are used and normalised.

Thermodynamic Considerations

Table S11: Standard Gibbs free energy for different metabolic reactions.

Electron donor	Electron acceptor	Product	Reaction ΔG_0' (kJ/mol)	Reference
Ammonium	Nitrite	N_2	–358	[6]
Ammonium	Electrode	N_2	-173.7	[7]
Hydroxylamine	Hydroxylamine	N_2	-227.9	[8]

Table S12: Theoretical ATP/e- and H+/e- R for Ammonium oxidation and Reduction Coupled electron transfer chain.

ΔG_0	ATP/e- ratio (maximum)	Proton translocation/mole ATP	H^+/e^- ratio		Assumed Energy transfer efficiency (%)	ATP/e- (Assumed)
			Max	Assumed		
-358	1.81	4	5.43	6	100	1.50
				5	83.3	1.25
				4	66.7	1.00
				3	50	0.75
				2	33.3	0.50
				1	16.7	0.25

Table S13: Theoretical ATP/e- and H+/e- for Ammonium oxidation Coupled with Reduction of Standard Hydrogen Electrode.

ΔG_0	ATP/e- ratio (maximum)	Proton translocation/mole ATP	H^+/e^- ratio		Assumed Energy transfer efficiency (%)	ATP/e- (Assumed)
			Max	Assumed		
-173	1.17	4	3.51	4	100	1.00
				3	75	0.75
				2	50	0.50
				1	25	0.25

Gap Filling

Some subsystems in the ANAMMOX metabolism had very poor annotation and required gapfilling and further investigation to ensure their functionality. The following table contains some of this information for the genes which were investigated.

Table S14: BLAST[9] alignment of important features not initially found using RAST annotation.

Enzyme	**Subunit**	**Feature ID**	**Closest UniProtKB/ Swiss-Prot (swissprot) BLAST result (%identity)**	**e-Value**	**Closest non ANAMMOX Non-redundant Protein sequence (nr) database result (%identity)**	**e-Value**
Reverse TCA specific genes						
Succinate dehydrogenase (quinol) 1.3.5.1	SdhA*					
	SdhB	KsCSTR_RS00725	Succinate dehydrogenase [ubiquinone] iron-sulfur	1e-61	Succinate dehydrogenase iron-sulfur subunit [Candidatus	2e-99

			subunit 2 Arabidopsis thaliana Q8LB02.2 (44.05%)		Marinimicrobia bacterium] 56.47%	
	SdhC	KsCSTR_RS18490	Succinate dehydrogenase 2 membrane subunit SdhC [Mycobacterium tuberculosis] (28.46%)	5e-09	Succinate dehydrogenase 2 membrane subunit SdhC [Candidatus Marinimicrobia bacterium] (48.21%)	9e-29
	SdhD*					
2-oxoglutarate synthase ec: 1.2.7.3-	KorA	KsCSTR_RS00370	2-oxoglutarate synthase subunit KorA [Archaeoglobus fulgidus] (36.52%)	2e-61	3-methyl-2-oxobutanoate dehydrogenase subunit VorB [Anaerobranca californiensis] WP_072905739.1 (61.10%)	2e-154
	KorB	KsCSTR_RS00365	2-oxoglutarate-ferredoxin oxidoreductase subunit beta [Methanocaldococcus jannaschii DSM 2661] (38.54%)	2e-39	Might have different name in database (oxoglutarate oxiedoreductase)	
Gluconeogenesis specific genes						
Pyruvate carboxylase ec:6.4.1.1	Single gene	KsCSTR_RS04340	Pyruvate carboxylase [Bacillus subtilis subsp. subtilis str. 168] Q9KWU4.1 (54.07%)	0.0	pyruvate carboxylase [Lentisphaera araneosa] WP_040914872.1 (65.80%)	0.0
Phosphoenolpyruvate carboxykinase (ATP) ec:4.1.1.49-	Single gene	KsCSTR_RS12330	Phosphoenolpyruvate carboxykinase (ATP) [Aeropyrum pernix K1] Q9YG68.2 (32.12%)	1e-58	TPA: phosphoenolpyruvate carboxykinase [Armatimonadetes bacterium] HHA15313.1 (57.06%)	0.0
fructose 1,6-bisphosphatase class 1 ec:3.1.3.11-	Single gene	KsCSTR_RS04100	Fructose-1,6-bisphosphatase class 1 [Chloroherpeton thalassium ATCC 35110] B3QWF5.1 (62.84%)	2e-146	fructose-1,6-bisphosphatase [Desulfovibrio magneticus str. Maddingley MBC34] EKO40391.1 (61.73%)	1e-141
glucose 6-phosphatase*						
Anaerobic carbon-monoxide dehydrogenase ec:1.2.7.4	Alpha copy 1	KsCSTR_RS03835	Carbon monoxide dehydrogenase 1 [Methanosarcina acetivorans C2A] Q8TKW2.1 (48.56%)	0.0		
	Alpha copy 2	KsCSTR_RS11645	Carbon monoxide dehydrogenase 1; Short=CODH 1 [Carboxydothermus hydrogenoformans Z-2901] P59934.3 (42.68%)	1e-166		

CO-methylating acetyl-CoA synthase ec:2.3.1.169-	Alpha	KsCSTR_RS03840	Carbon monoxide dehydrogenase/acetyl-CoA synthase subunit alpha [Moorella thermoacetica] P27988.1 (46.56%)	0.0	CO dehydrogenase/CO-methylating acetyl-CoA synthase complex subunit beta [Deferrisoma camini] WP_025323519.1 (63.13%)	0.0
5-methyltetrahydrofolate:corrinoid/iron-sulfur proteinCo-methyltransferase ec:2.1.1.258-		KsCSTR_RS03870	5-methyltetrahydrofolate:corrinoid/iron-sulfur protein co-methyltransferase [Moorella thermoacetica] Q46389.2 (45.00%)	5e-82	methyltetrahydrofolate cobalamin methyltransferase [Acetohalobium arabaticum] WP_013278258.1 (47.89%)	8e-85
	small subunit (probably related)	KsCSTR_RS03865	Corrinoid/iron-sulfur protein small subunit [Moorella thermoacetica] Q07341.2 (51.26%)	3e-111	acetyl-CoA decarbonylase/synthase complex subunit delta [Sporomusa acidovorans] WP_094607893.1 (53.23%)	3e-118
	large subunit (probably related)	KsCSTR_RS03850	Corrinoid/iron-sulfur protein large subunit; Short=C/Fe-SP large subunit [Moorella thermoacetica] Q07340.2 (46.26%)	3e-132	acetyl-CoA decarbonylase/synthase complex subunit gamma [Thermodesulfitimonas autotrophica] WP_123928501.1 (52.48%)	3e-159
Sulphur Metabolism						
Sulfate adenylyltransferase ec:2.7.7.4-		KsCSTR_RS08580	Sulfate adenylyltransferase B8D0S5.1 [Halothermothrix orenii H 168] (60.94%)	4e-173		
Adenylyl-sulfate kinase ec:2.7.1.25	Copy 1	KsCSTR_RS04455	Adenylyl-sulfate kinase Q4L9E6.1 [Staphylococcus haemolyticus JCSC1435] (62.83%)	5e-87		
	Copy 2	KsCSTR_RS10510	Adenylyl-sulfate kinase B7K5B1.1 [Rippkaea orientalis PCC 8801] (46.93%)	6e-52		
Phosphoadenylyl-sulfate reductase (thioredoxin) ec:1.8.4.8		KsCSTR_RS10955	Adenosine 5'-phosphosulfate reductase A0R0W2.1 [Mycolicibacterium smegmatis MC2 155] (35.51%)	6e-42		
1.12.98.4 Anaerobic sulfite reductase subunit A		KsCSTR_RS11265	Sulfhydrogenase 1 subunit beta Q8U2E5.1 [Pyrococcus furiosus DSM 3638] (35.29%)	1e-63		

Amino Acid Metabolism						
ec:4.3.1.1-Aspartate ammonia-lyase.		KsCSTR_RS01220	Aspartate ammonia-lyase; Short=Aspartase [Helicobacter pylori J99] (49%)	6e-144		
ec:2.6.1.83-LL-diaminopimelate aminotransferase.		KsCSTR_RS09610	LL-diaminopimelate aminotransferase [Thermodesulfatator indicus] (48%)	8e-103		

Nucleic Acids

In the ModelSEED system the RNA and DNA in the cell have their own ID (cpd17043[c0] and cpd17042[c0]) respectively. The relative molar amounts of each in the genome are used to create the following chemical reactions:

RNA Synthesis:

0.05001103 cpd00018[c0] + 0.02409133 cpd00126[c0] + 0.02429681 cpd00206[c0] + 0.04945548 cpd00091[c0] <=> cpd17043[c0]

DNA Synthesis:

0.02784256 cpd00115[c0] + 0.01354480 cpd00356[c0] + 0.01354480 cpd00241[c0] + 0.02784256 cpd00357[c0] <=> cpd17042[c0]

Ladderanes

Since there is no established pathway for glycerol ether ladderanes their biosynthesis is modelled after an established diether biosynthetic pathway [10]. Bacteriohopanetetrol also did not appear to have a well-established biosynthesis so it was considered as identical to diplopterol in the model's biomass.

It is generally understood that ladderanes are derived from fatty acids with the same number of carbon atoms and somehow rearranged and dehydrated. The carrier for the hydrogen resulting from dehydrogenation has not been confirmed but it is likely flavin adenine dinucleotide (FAD) which can accept $2H^+$ and $2e^-$ to become FADH.

Two ladderane fatty acids need to be synthesised for this model: C18 and C20 ladderane:

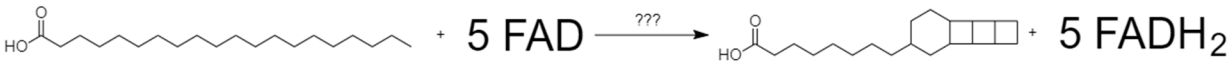

Figure S1: hypothetical ladderane synthesis from C20:0 fatty acid.

cpd03848[0] + 5 cpd00015[c0] <=> cpd10002[c0] + 5 cpd00982[c0]

It is recognised that this is an approximation for this reaction since there isn't firm proof for how the biosynthesis takes place *in vivo.*

Cell Wall Components

Page 123 of physiology of the bacterial cell by F.Niedhart [11] describes typical needs for a gram of biomass cell wall to be made. The example pathway used to gapfill the biosynthesis of muropeptides is found in the Metacyc database [12] "peptidoglycan biosynthesis I (meso-diaminopimelate containing)".

Calculation of *Ca. Kuenenia stuttgartiensis* Cell Composition

The shape of *K. Stuttgartiensis* cell is reported as spherical.

The diameter of a *K. Stuttgartiensis* Cell is on average 0.8µm [13]

The volume of one *K. Stuttgartiensis* cell is: $\frac{4}{3}\pi r^3 = \frac{1}{6}\pi D^3 = \frac{1}{6} \times \pi \times (0.8)^3 = 0.268 \mu m^3$

E.coli, also a gram negative bacterium, generally have a density of 1.1 g/ml [14].

The mass of one cell is therefore $1.1\ g/ml \times 0.268\ \mu m^3 \times 10^{-12} ml\ \mu m^{-3} = 2.95 \times 10^{-13} g$

Typically, a bacterial cell is 70% water by mass, so the dry mass of a cell is:

$\frac{2.95 \times 10^{-13}}{1-0.7} = 8.847 \times 10^{-13} g$

The dry mass percentage composition of DNA is therefore the total mass of a chromosome divided by the dry mass of a cell:

$$\frac{Nucleotide\ count \times Molecular\ weights}{single\ cell\ dry\ mass \times Avogadro's\ number}$$

$$\frac{1297860 \times 491.2 + 905231 \times 467.2 + 905231 \times 507.2 + 1297860 \times 482.2}{8.847 \times 10^{-13} \times 6.022 \times 10^{23}} = 0.0403 = 4.03\%$$

Electron Transport chain

The electron transport chain has previously been described and contains respiratory complexes I, II, III and IV [15]. Simulations using electron transport chain setup as previously described[15] did not function correctly as they produced thermodynamically unfeasible cycles when oxidising nitrite to nitrate.

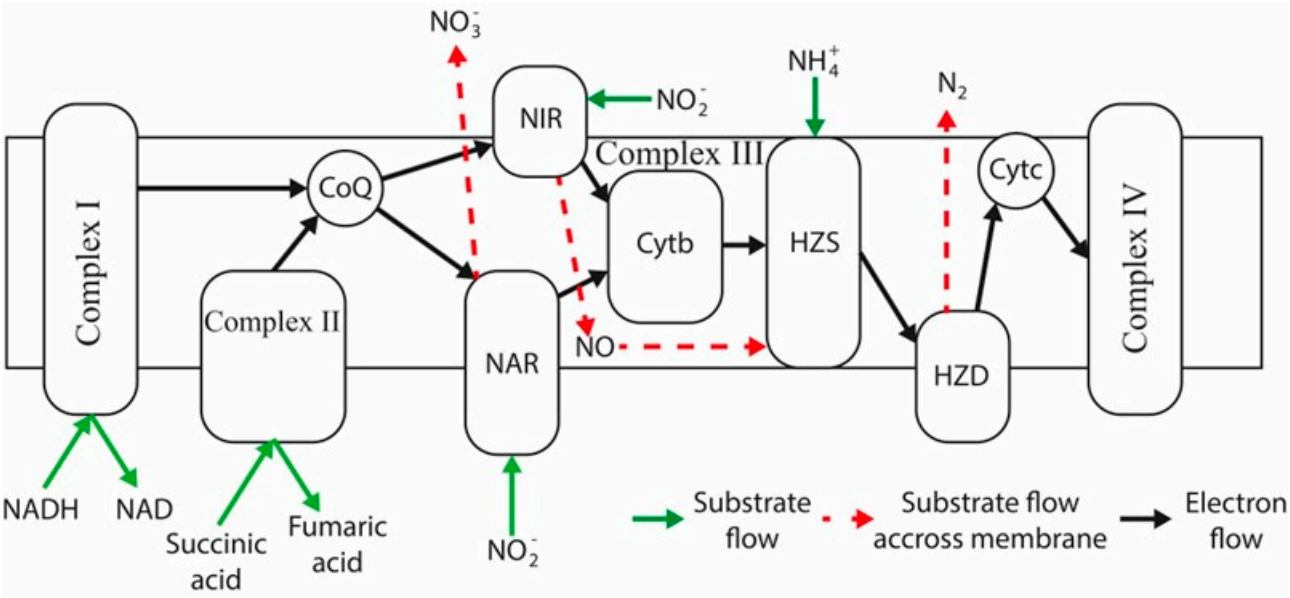

Figure S2:iRB399 reconstruction of the electron transport chain [15]

Here the NAR enzyme is problematic since it isn't entirely clear how this should function in the metabolic model. The original proposition was that it is used in carbon fixation but this cannot be true since it is thermodynamically unfeasible. Furthermore, ANAMMOX have been shown to grow in absence of nitrite and using nitric oxide as a sole electron acceptor and without producing nitrate[16]. Therefore, it is more likely that something else is taking place.

Calculation of Maximum Energy Transfer Efficiency (ATP/e^-) and Proton Translocation Stoichiometry (H^+/e^- ratio) of *Ca. Kuenenia Stuttgartiensis* Electron Transport Chain.

The theoretical maximum ATP/e^- ratio, $(\eta_{ATP}/\eta_e)_{max}$ can be determined from the following equation [17]:

$$\left(\eta_{ATP}/\eta_e\right)_{max} = {\Delta E_0{}' F}/{\Delta G_p{}'} \quad \text{(S1)}$$

Where F is the Faraday constant (96,500 J/mol .V), ΔE_0 is the difference in standard redox potential between the electron donor and acceptor and ΔG_p' is the free energy of phosphorylation reaction at pH 7 and physiological condition.

Since $\Delta G_0' = -nF\Delta E_0{}'$

Therefore, $\left(\eta_{ATP}/\eta_e\right)_{max} = {\Delta G_0{}' F}/{n\Delta G_p{}'}$ (S2)

Where n is the number of electrons transferred in the reaction.

ΔG_p' at physiological conditions can be calculated from the free energy of the phosphorylation reaction at standard conditions and pH 7 ($\Delta G_{0,p}$) using the following equation:

$$\Delta G_p' = \Delta G_0' + RT \ln\left(\frac{[ATP]}{[ADP][P_i]}\right) \quad \text{(S3)}$$

Where, $\Delta G_{0,p}'$ = 32 kJ/mol [18], R is the universal gas constant having a value of 8.314 J/mol.K and T is the absolute temperature, 310.15K at 37ºC which is the temperature GAM was measured at[19].

Assuming that the concentrations of ATP and ADP are equal, and that the concentration of P_i is 1 mM, then the calculated value of ΔG_p' using equation (S3) is 49.46 kJ/mol.

The average standard free energy for the nitrite and ammonium ANAMMOX reaction is ΔG_0'=-358 kJ/mol (Table S11).

Therefore, theoretical maximum ATP/e^- using equation (S2) is:

$$\left(\eta_{ATP}/\eta_e\right)_{max} = \frac{358}{4 \times 49.46} = 1.81$$

Assuming the number of H^+ translocated across the membrane during the phosphorylation of ADP is 4, we obtain the theoretical maximum H^+/e^- is 5.43. Referring to Table S12 this means the H^+/e^- ratio can be either 5 or 6. This means the process can have a theoretical efficiency of 83.3% however this is uncharacteristic of anaerobes and when applied to the model results in GAM being much higher than anything reported in literature. A thermodynamic efficiency of 16.7% and a H^+/e^- ratio of 1 is chosen.

Since the ATP/e^- value (0.25) corresponds to 1 H^+/e^- this means that 1 mole of NH_3 consumed with nitrite as the electron sink corresponds to 1.20 ATP/NH_3 and depending on efficiency might be as high as 7.24. When considering transportation costs and that in the cell this figure becomes 0.75 since nitrite is transported into the cell via proton symport.

For EET this is calculated using the half equation using only ammonium:

$$NH_4^+ \xrightarrow{+0.6V\ vs.SHE} 0.5N_2 + 4H^+ + 3e^-$$

Now Gibbs free energy can be calculated:

$$\Delta G_0' = -nF\Delta E_0{}'$$

$$\Delta G_0' = -3 \times 96{,}500 \times 0.6 = -173.700\ KJ/mol$$

Now to calculate the maximum amount of ATP that can be derived from those electrons:

$$\left(\eta_{ATP}/\eta_e\right)_{max} = \frac{173.7}{3 \times 49.46} = 1.171$$

Assuming the number of H+ translocated across the membrane during the phosphorylation of ADP is 3, the theoretical maximum H+/e- is 3.51. Referring to Table S13 this means the H+/e- ratio should be either 2 or 3. This means the process can have a theoretical efficiency of 75% however this is uncharacteristic of anaerobes so 25% efficiency is chosen at a H+/e- ratio of 1.

Calculation of GAM and NGAM

Non-Growth Associated Maintenance energy for *K. Stuttgartiensis* is likely to be very similar to that of *Ca. Brocadia Sinica*. The intercept on the Y axis is the amount of NH4 required for maintenance in terms of NH4 per unit protein. This can be converted to consumption of NH4 per unit biomass and since the electron transport chain has an efficiency of 0.75 ATP/NH4 consumed the NGAM is calculated as:

$$NGAM = 1.26 \times 0.6 \times 0.75 = 0.5625 mmolATP(g.DCW)^{-1}h^{-1}$$

For another species of ANAMMOX bacteria, "Ca. Scalindua sp." NGAM was measured as 0.8255 mmol NH_4^+g-protein^{-1}h^{-1}[19]. Since the cell has a mass fraction of 0.6g.protein/g.biomass the consumption of NH_4^+ per gram of biomass is:

$$NGAM = 0.8255 \times 0.6 \times 0.75 = 0.3714 mmolATP(g.DCW)^{-1}h^{-1}$$

Since ATP is produced at a rate of 0.75 ATP/NH_3 the maintenance energy (NGAM) is therefore:
$2.1 \times 1.82 = 3.82 \pm 0.21 mmolATPg.biomass^{-1}h^{-1}$

In iRB399 the NGAM is kept as the lower figure, 0.3714 and the NGAM reaction is:

The specific uptake of ammonia of an ANAMMOX species, *Ca. Broccadia sinica* has been previously determined as is 990.05 NH_4^+g-protein^{-1}h^{-1}[19]. By adjusting the GAM in iRB399 to achieve this relationship the GAM was found to be 363.27 ATP/g-biomass.

iRB399 Biomass Equation

0.31152673 cpd00035[c0] + 0.06337841 cpd00084[c0] + 0.23592979 cpd00041[c0] + 0.32127661 cpd00023[c0] + 0.20832589 cpd00066[c0] + 0.31027163 cpd00033[c0] + 0.09760276 cpd00119[c0] + 0.37841277 cpd00322[c0] + 0.34888882 cpd00039[c0] + 0.42827185 cpd00107[c0] + 0.11216525 cpd00060[c0] + 0.21423151 cpd00132[c0] + 0.17104691 cpd00129[c0] + 0.13755402 cpd00053[c0] + 0.21931425 cpd00051[c0] + 0.28088067 cpd00054[c0] + 0.24589578 cpd00161[c0] + 0.29402182 cpd00156[c0] + 0.04838371 cpd00065[c0] + 0.16570235 cpd00069[c0] + 1.00000000 cpd17042[c0] + 1.00000000 cpd11613[c0] + 0.009379269 cpd15599b[c0] + 0.040827407 cpd03847[c0] + 0.015723589 cpd15599[c0] + 0.060437546 cpd00214[c0] + 0.047977819 cpd15599[c0] + 0.029387755 cpd01080[c0] + 0.06581157 cpd10002[c0] + 0.00705573 cpd00559[c0] + 0.099406932 cpd05269a[c0] + 0.001469559 cpd03750[c0] + 0.005362177 cpd05269b[c0] + 0.011618051 cpd05269c[c0] + 0.004256728 cpd05269d[c0] + 0.004408677 cpd03750[c0] + 0.075941247 cpdM3[c0] + 0.012928938 cpdM4[c0] + 0.020728436 cpdM2[c0] + 0.026101822 cpdD43[c0] + 0.663162359 cpd00205[c0] + 0.095539426 cpd00254[c0] + 0.003236217 cpd10516[c0] + 0.003007556 cpd00063[c0] + 0.013505025 cpd00009[c0] + 0.000861943 cpd00012[c0] + 0.000194986 cpd15499[c0] + 0.000296988 cpd00201[c0] + 0.013082729 cpd00003[c0] + 0.003771727 cpd00018[c0] + 0.002420509 cpd00002[c0] + 0.002079208 cpd00008[c0] + 0.000564756 cpd00046[c0] + 0.000756348 cpd00006[c0] + 0.000438322 cpd00052[c0] + 0.000447674 cpd00126[c0] + 0.000350607 cpd00038[c0] + 0.000209895 cpd00096[c0] +

0.000169949 cpd00005[c0] + 0.000159019 cpd00031[c0] + 363.27 cpd00002[c0] + 363.27 cpd00001[c0] <=> 363.27 cpd00008[c0] + 363.27 cpd00009[c0] + 363.27 cpd00067[c0]

Programs

The programs written to carry out the figure creation and analysis in this paper can be found at:

https://github.com/rmnsgrt/metabolic_modelling.git

Instructions for using the programs are also included in the descriptions for each program and further details are included in the comments of the program for spaces that require input.

Bibliography

1. Lieven, C.; Beber, M.E.; Olivier, B.G.; Bergmann, F.T.; Ataman, M.; Babaei, P.; Bartell, J.A.; Blank, L.M.; Chauhan, S.; Correia, K.; et al. MEMOTE for Standardized Genome-Scale Metabolic Model Testing. *Nature Biotechnology* **2020**, *38*, 272–276, doi:10.1038/s41587-020-0446-y.
2. Soga, T.; Ohashi, Y.; Ueno, Y.; Naraoka, H.; Tomita, M.; Nishioka, T. Quantitative Metabolome Analysis Using Capillary Electrophoresis Mass Spectrometry. *Journal of Proteome Research* **2003**, *2*, 488–494, doi:10.1021/pr034020m.
3. Strous, M.; Kuenen, J.G.; Jetten, M.S.M. Key Physiology of Anaerobic Ammonium Oxidation. *Applied and Environmental Microbiology* **1999**, *65*, 3248–3250, doi:10.1128/aem.65.7.3248-3250.1999.
4. Neumann, S.; Wessels, H.J.C.T.; Rijpstra, W.I.C.; Sinninghe Damsté, J.S.; Kartal, B.; Jetten, M.S.M.; van Niftrik, L. Isolation and Characterization of a Prokaryotic Cell Organelle from the Anammox Bacterium Kuenenia Stuttgartiensis. *Molecular Microbiology* **2014**, *94*, 794–802, doi:10.1111/mmi.12816.
5. Van Teeseling, M.C.F.; Mesman, R.J.; Kuru, E.; Espaillat, A.; Cava, F.; Brun, Y.V.; Vannieuwenhze, M.S.; Kartal, B.; Van Niftrik, L. Anammox Planctomycetes Have a Peptidoglycan Cell Wall. *Nature Communications* **2015**, *6*, 6878, doi:10.1038/ncomms7878.
6. In 't Zandt, M.H.; De Jong, A.E.E.; Slomp, C.P.; Jetten, M.S.M. The Hunt for the Most-Wanted Chemolithoautotrophic Spookmicrobes. *FEMS Microbiology Ecology* **2020**, *94*, fiy064, doi:10.1093/femsec/fiy064.
7. Shaw, D.R.; Ali, M.; Katuri, K.P.; Gralnick, J.A.; Reimann, J.; Mesman, R.; van Niftrik, L.; Jetten, M.S.M.; Saikaly, P.E. Extracellular Electron Transfer-Dependent Anaerobic Oxidation of Ammonium by Anammox Bacteria. *Nature Communications* **2020**, *11*, 2058, doi:10.1038/s41467-020-16016-y.
8. Oshiki, M.; Ali, M.; Shinyako-Hata, K.; Satoh, H.; Okabe, S. Hydroxylamine-Dependent Anaerobic Ammonium Oxidation (Anammox) by "Candidatus Brocadia Sinica." *Environmental microbiology* **2016**, *18*, 3133–3143, doi:10.1111/1462-2920.13355.
9. Altschul, S.F.; Gish, W.; Miller, W.; Myers, E.W.; Lipman, D.J. Basic Local Alignment Search Tool. *Journal of Molecular Biology* **1990**, *215*, doi:10.1016/S0022-2836(05)80360-2.
10. Magnusson, C.D.; Haraldsson, G.G. Ether Lipids. *Chemistry and Physics of Lipids* **2011**, *164*, 315–340, doi:10.1016/j.chemphyslip.2011.04.010.
11. Neidhardt, F.C.; Ingraham, J.L.; Schaechter, M. *Physiology of the Bacterial Cell. A Molecular Approach*; 1992; Vol. 20;.
12. Caspi, R.; Altman, T.; Billington, R.; Dreher, K.; Foerster, H.; Fulcher, C.A.; Holland, T.A.; Keseler, I.M.; Kothari, A.; Kubo, A.; et al. The MetaCyc Database of Metabolic Pathways and Enzymes and the BioCyc Collection of Pathway/Genome Databases. *Nucl. Acids Res.* **2014**, *42*, D459–D471, doi:10.1093/nar/gkt1103.
13. Van Niftrik, L.; Geerts, W.J.C.; Van Donselaar, E.G.; Humbel, B.M.; Webb, R.I.; Fuerst, J.A.; Verkleij, A.J.; Jetten, M.S.M.; Strous, M. Linking Ultrastructure and Function in Four Genera

of Anaerobic Ammonium-Oxidizing Bacteria: Cell Plan, Glycogen Storage, and Localization of Cytochrome c Proteins. *Journal of Bacteriology* **2008**, *190*, 708–717, doi:10.1128/JB.01449-07.
14. Lewis, C.L.; Craig, C.C.; Senecal, A.G. Mass and Density Measurements of Live and Dead Gram-Negative and Gram-Positive Bacterial Populations. *Applied and Environmental Microbiology* **2014**, *80*, 3622–3631, doi:10.1128/AEM.00117-14.
15. Wang, S.; Guo, J.; Lian, J.; Ngo, H.H.; Guo, W.; Liu, Y.; Song, Y. Rapid Start-up of the Anammox Process by Denitrifying Granular Sludge and the Mechanism of the Anammox Electron Transport Chain. *Biochemical Engineering Journal* **2016**, *115*, 101–107, doi:10.1016/j.bej.2016.09.001.
16. Hu, Z.; Wessels, H.J.C.T.; van Alen, T.; Jetten, M.S.M.; Kartal, B. Nitric Oxide-Dependent Anaerobic Ammonium Oxidation. *Nature Communications* **2019**, *10*, 1244, doi:10.1038/s41467-019-09268-w.
17. Kröger, A.; Biel, S.; Simon, J.; Gross, R.; Unden, G.; Lancaster, C.R.D. Fumarate Respiration of Wolinella Succinogenes: Enzymology, Energetics and Coupling Mechanism. *Biochimica et Biophysica Acta - Bioenergetics* **2002**, *1553*, 23–38, doi:10.1016/S0005-2728(01)00234-1.
18. Thauer, R.K.; Jungermann, K.; Decker, K. Energy Conservation in Chemotrophic Anaerobic Bacteria. *Bacteriological Reviews* **1977**, *41*, 100–180, doi:10.1128/mmbr.41.1.100-180.1977.
19. Okabe, S.; Kamigaito, A.; Kobayashi, K. Maintenance Power Requirements of Anammox Bacteria “Candidatus Brocadia Sinica” and “Candidatus Scalindua Sp.” *ISME Journal* **2021**, 3566–3575, doi:10.1038/s41396-021-01031-8.